

# PCCP

Accepted Manuscript



This is an *Accepted Manuscript*, which has been through the Royal Society of Chemistry peer review process and has been accepted for publication.

*Accepted Manuscripts* are published online shortly after acceptance, before technical editing, formatting and proof reading. Using this free service, authors can make their results available to the community, in citable form, before we publish the edited article. We will replace this *Accepted Manuscript* with the edited and formatted *Advance Article* as soon as it is available.

You can find more information about *Accepted Manuscripts* in the [Information for Authors](#).

Please note that technical editing may introduce minor changes to the text and/or graphics, which may alter content. The journal's standard [Terms & Conditions](#) and the [Ethical guidelines](#) still apply. In no event shall the Royal Society of Chemistry be held responsible for any errors or omissions in this *Accepted Manuscript* or any consequences arising from the use of any information it contains.



Journal Name

ARTICLE TYPE

Cite this: DOI: 10.1039/xxxxxxxxxx

## Formic acid oxidation on platinum: a simple mechanistic study<sup>†</sup>

Kathleen A. Schwarz,<sup>\*a</sup> Ravishankar Sundararaman,<sup>b</sup> Thomas P. Moffat,<sup>c</sup> and Thomas C. Allison<sup>c</sup>

Received Date  
Accepted Date

DOI: 10.1039/xxxxxxxxxx

www.rsc.org/journalname

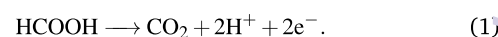
The oxidation of small organic acids on noble metal surfaces under electrocatalytic conditions is important for the operation of fuel cells and is of scientific interest, but the basic reaction mechanisms continue to be a matter of debate. Formic acid oxidation on platinum is one of the simplest of these reactions, yet even this model system remains poorly understood. Historically, proposed mechanisms for the oxidation of formic acid involve the acid molecule as a reactant, but recent studies suggest that the formate anion is the reactant. *Ab initio* studies of this reaction do not address formate as a possible reactant, likely because of the difficulty of calculating a charged species near a charged solvated surface under potential control. Using the recently-developed Joint Density Functional Theory (JDFT) framework for electrochemistry, we perform *ab initio* calculations on a Pt(111) surface to explore this reaction and help resolve the debate. We find that when a formate anion approaches the platinum surface at typical operating voltages, with H pointing towards the surface, it reacts to form CO<sub>2</sub> and adsorbed H with no barrier on a clean Pt surface. This mechanism leads to a reaction rate proportional to formate concentration and number of available platinum sites. Additionally, high coverages of adsorbates lead to large reaction barriers, and consequently, we expect the availability of metal sites to limit the experimentally observed reaction rate.

### 1 Introduction

Formic acid oxidation has been a topic of recent interest due to its key role in the operation of direct formic acid fuel cells,<sup>1–7</sup> which are candidates for portable power sources.<sup>8</sup> Additionally, formic acid is an intermediate in the methanol oxidation process relevant for the operation of methanol fuel cells.

The direct formic acid oxidation reaction at Pt surfaces under electrocatalytic conditions has been widely studied by theoretical<sup>9–12</sup> and experimental<sup>13–30</sup> means, but some fundamental questions about the reactive species and the reaction mechanism

remain unresolved. Complete oxidation yields CO<sub>2</sub> and protons:



The mechanism of the direct pathway to HCOOH oxidation (i.e. without forming CO as an intermediate) remains a source of conflict. A number of reaction mechanisms and rate equations<sup>13,14,24,31,32</sup> have been proposed based on computational predictions and experimental observations, yet there is no consensus with regard to either the observed facts or their interpretation. Even the active reactant is debated, with the most recent evidence suggesting that it is formate rather than formic acid.<sup>25,33</sup> The correct rate equations are difficult to identify because they are a function of pH, potential, and surface coverage of both potential intermediates and spectator species, and include contributions from multiple reaction pathways. The rate's dependence on these variables is difficult to deconvolve. For instance, experimental observation of the pH effect has been inconsistent, with

<sup>a</sup> National Institute of Standards and Technology, Material Measurement Laboratory, 100 Bureau Dr, Gaithersburg, MD, USA. E-mail: kas4@nist.gov

<sup>b</sup> The Joint Center for Artificial Photosynthesis, California, USA.

<sup>c</sup> National Institute of Standards and Technology, Material Measurement Laboratory, 100 Bureau Dr, Gaithersburg, MD, USA.

<sup>†</sup> Electronic Supplementary Information (ESI) available: [details of any supplementary information available should be included here]. See DOI: 10.1039/b000000x/

groups finding an increase in maximum oxidation current with increasing pH up to  $\text{pH} = 2$  in proportion to the concentration of formate.<sup>25,34,35</sup> However, one group found that the largest current maximum occurs at a pH equal to the  $\text{pK}_a$  of formate,<sup>25,33</sup> while another group found that it plateaus at a pH above the  $\text{pK}_a$  of formate.<sup>35</sup> Experimental interpretation is complicated by the fact that the surface coverage of adsorbates changes with both potential and pH, and that the experiments appear to be strongly influenced by the anions used in the electrolyte.<sup>35</sup>

Density functional theory (DFT) studies provide a way to separately consider the variables that affect formic acid oxidation on platinum and their contributions to the reaction mechanism, but the methodology for making contact with experiments is still a field of active development. The need to understand the role that voltage, electrolyte, catalyst surface conditions, and pH play in the formic acid oxidation reaction means that great care must be taken when performing and interpreting these calculations.

Different approaches for overcoming these difficulties have led computational studies to reach differing conclusions. For instance, one study suggests a dual mechanism,<sup>12</sup> while others argue that there are three competing pathways<sup>36</sup> for the reaction of formic acid. The studies do not agree on the orientation of the molecule, with some demonstrating that CH-down formic acid (i.e. the H faces the catalyst surface) is key to reaction<sup>10,24</sup>, and others arguing for the CO-down configuration.<sup>12</sup> The mechanisms almost all include an adsorbed formic acid or formate precursor,<sup>10,36</sup> leading to large reaction barriers.<sup>37</sup> The barriers associated with these reactions on pristine Pt surfaces are  $\sim 1$  eV which, even after accounting for vibrational effects, are much higher than the apparent activation energies found experimentally.<sup>34</sup> Only recently has a computational study found low barriers associated with the reaction of formic acid with Pt surfaces, but these surfaces are modified by adatoms,<sup>38</sup> and the authors attribute the low barrier to the adsorption of formic acid on the adatoms.

To correctly evaluate the reaction free energies, barrier heights, and free energy shifts due to solvation, adsorption to the catalyst, chemical potential, and voltage must be taken into consideration, as illustrated in Figure 1.\* From right to left, the diagram depicts the relative energies of the products and the possible reactants. The diagram shows the large solvation energy associated with formate. Solvation effects are particularly important for the formate oxidation reaction because the charged reactant, formate, is considerably more stabilized by solvation than the neutral products, a surface-bound hydrogen and non-polar  $\text{CO}_2$ . However, if

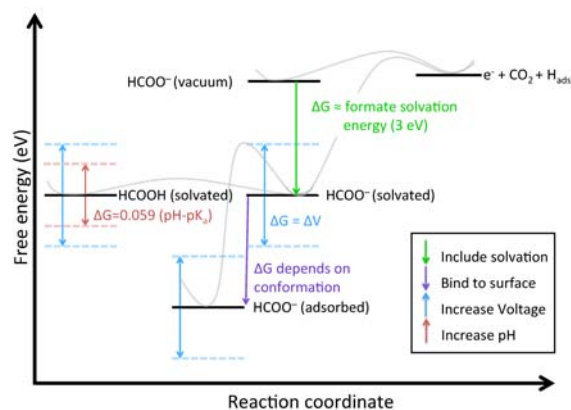


**Fig. 1** Illustration of the relative free energies of the products and possible reactants in the formic acid oxidation reaction on a clean Pt surface. The y-axis represents the free energies of the systems above, with the Pt slab energy included in each state, and with the voltage and solvation of the slab changing as appropriate. Additionally, the states with formate and that with  $\text{CO}_2$  have the energy of the proton that is included implicitly (which gives rise to the shift seen with pH relative to the formic acid). For conceptual simplicity, the voltage in this figure is given relative to the reversible hydrogen electrode.

the formate is adsorbed rather than solvated, the adsorbed conformation is lower in energy than that of the solvated formate, with its relative energy dependent on configuration. The relative free energies of solvated formic acid and formate vary with pH, and become equal at the  $\text{pK}_a$  of formic acid. With increasing electrode potential, the energies of the products decrease relative to the reactants, because one of the products is an electron (which has an energy equal to that of the Fermi level).

All these factors that shift the free energies must be considered to correctly assess the relative reaction free energies. For instance Ref. 10 finds that the reaction barrier for monodentate formate to form  $\text{CO}_2$  on a platinum slab in vacuum is only 0.05 eV, whereas the solvated monodentate formate has a barrier of 0.83 eV. The authors argue that the initial state, monodentate formate, is stabilized by solvation, whereas the final state,  $\text{CO}_2$ , is poorly solvated and is not as stabilized by solvation. The transition state is similar to the final state, and so they report a high barrier to reaction. This is misleading because much of the barrier is most likely due to the change in the reaction energy, associated with the difference between the solvated initial state, and the poorly solvated final state. If the voltage is then considered, as the voltage is increased, the oxidation reaction becomes more favorable, and the transition state energy most likely also becomes closer to the initial state energy. The paper's use of a slab calculation at fixed charge precludes oxidation, the loss of an electron, with the associated free energy contribution equal to the energy value of

\*We note that the free energies used in this paper are the Gibbs free energies with respect to atomic species, and grand free energy with respect to the electrons because the number of atoms is fixed, but the electron chemical potential (instead of the number of electrons) should be fixed for these calculations.

the Fermi level. Instead, the charge of the whole system remains constant, and the voltage, which is not reported, changes uncontrollably during the reaction. The gap between the experimental reality of a fixed-voltage experiment and a fixed-charge calculation (that does not account for changes in potential) limits the applicability of studies such as these.

This example illustrates the challenges that electrochemical systems present for computational approaches. However, while traditional DFT does not provide a framework for addressing the free energy shifts as conditions in the experimental environment change, approximations and approaches for addressing these problems is an area of recent growth.<sup>39–43</sup> In these methods, different approximations are applied to model the half-cell. The Neurock group,<sup>43</sup> for instance, creates a half-cell in which the slab is at a fixed potential, and the cell is neutralized by an evenly-distributed background charge. The Nørskov group,<sup>41</sup> takes another approach, using protons as explicit countercharges to neutralize a charged cell.

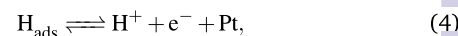
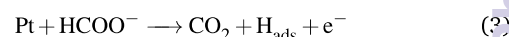
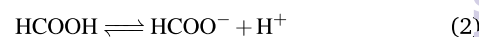
Here, we apply another approach<sup>40</sup> to examine formic acid oxidation on platinum. This method uses a continuum dielectric with ionic screening to both solvate the slab and neutralize the half cell. Unlike other approaches,<sup>43</sup> the neutralizing background charge is confined to the (implicit) fluid, rather than being spread evenly across the slab, reactants, and explicit fluid. Additionally, it does not require the specific placement of explicit countercharges.<sup>41</sup>

This approach relies on the framework of Joint Density Functional Theory<sup>44,45</sup> to treat the solvation effects and system charge. The key ansatz of JDFT is that the exact free energy of a system can be partitioned into the free energy of the solute, the free energy of the solvent, and a coupling term between the two. In practice, solvation models<sup>46–48</sup> have been developed that provide approximations for these terms, and here we apply one such solvation model, which has been applied to other electrochemical systems.<sup>46</sup>

Electrochemical systems are difficult to properly solvate computationally. Explicit water requires thermodynamic sampling through molecular dynamics simulations, and the water structure at the surface-electrolyte interface is voltage-dependent. Additionally, the ionic components of the electrolyte are important for the formation of the electrical double layer, and must also be included. The use of the screened dielectric continuum fluid eliminates the need for thermodynamic sampling, allowing ionic components to be implicitly included, and the charge distribution in the implicit fluid adjusts as a function of voltage. The ionic screening also allows for both a charged species and a charged surface to be included in the calculation, without unphysically long Coulomb interactions between unit cell images in the DFT calculation that would be present without an electrolyte. The use of ionic screening allows us to perform the calculations at a fixed

electron chemical potential, instead of using a fixed charge correction scheme (such as the computational hydrogen electrode, Ref. 41), so that the charge of the surface can change as the reaction proceeds. This means that the voltage is set in the calculation, and the oxidation reaction can be intuitively examined at a fixed voltage as the charge in the system changes, rather than trying to correct for excess charge trapped in the slab.

The aim of this article is to elucidate the mechanism of the formic acid oxidation reaction on Pt(111) by identifying: the reactive species, the species' orientation relative to the surface, the barrier to reaction, and the effects of surface adsorbates on reaction barriers. We also evaluate our proposed mechanism on the Au(111) surface to assess the generality of the reaction mechanism. We rigorously include electrochemically relevant components of the calculation, including charged species, an approximate double layer, and voltage effects following previously established methodology.<sup>40</sup> We explore the reactions of formic acid and formate on a Pt(111) surface, and detail how the energetics change as a function of pH, voltage, and solvation model. Our calculations support the following mechanism for formic acid oxidation on a pristine Pt surface:



with Pt representing an available Pt site, and with the formate oriented as illustrated in Figure 2.

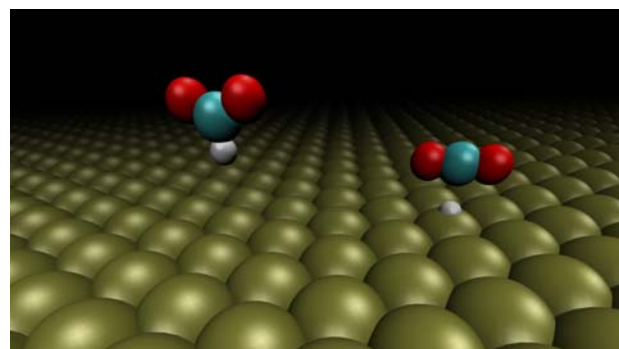


**Fig. 2** Formate approaching Pt(111) H-down (left), and reacting to form  $\text{CO}_2$  and a bound hydrogen (right).

## 2 Computational Details

We performed calculations using the code JDFTx,<sup>49</sup> with norm-conserving pseudopotentials at a plane-wave cutoff of 30 Hartree and the Perdew-Burke-Ernzerhof (PBE) exchange-correlation functional.<sup>50</sup> Following previously established system size convergence,<sup>12,36</sup> we used 3 layers of Pt in a  $3 \times 3$  unit cell with a  $2 \times 2$

gamma-centered  $k$ -point mesh. The bottom layer was fixed with a bond distance equal to that of the converged Pt bulk calculation, at 2.786 Å. A dielectric continuum with Debye screening was used to model the fluid,<sup>46</sup> with an ionic strength corresponding to 1 mol/L of both cations and anions. The fluid region between slabs was well-converged, with an inter-slab distance of 25.75 Å. To evaluate inter-slab interactions, the Coulomb-truncated<sup>51,52</sup> energy was compared to that of the untruncated calculation, and the energy of the formate on bare Pt changed by less than 1 milli-Hartree. All calculations were performed using the grand canonical ensemble for the electrons, using a fixed electron chemical potential<sup>53</sup> as a way to reduce finite size errors associated with charging the metal slab. Estimated free energies (as detailed in Ref. 46) are reported relative to the standard hydrogen electrode (SHE), using 4.44 V as the absolute level of SHE below the vacuum level.<sup>†</sup>

We note that an interesting subtlety of these calculations is that the Fermi level of a given calculation is fixed. We assume that the species are close enough to the surface so that the Fermi level does not change appreciably in the region of interest.<sup>‡</sup> This assumption has the consequence that we rely on the voltage lying between the HOMO and LUMO energy levels of the molecule or ion of interest. If this is not the case, the molecule or ion could have a different charge state than we expect, and could be unstable near the electrode. We calculated the HOMO of the formate, and it corresponds to an energy level equal to 0.65 V vs. SHE (and that of formic acid is considerably higher), so we are confident that formate and formic acid are in their correct charge states for these calculations.<sup>§</sup>

### 3 Results

Here, we explore Reaction 3, the reaction of formate on Pt(111) to produce an adsorbed hydrogen, an electron, and CO<sub>2</sub>. Using approximate free energy calculations, we compare the reactivity of formate in the CH-down configuration to that of formic acid in the same orientation, and we evaluate the role of pH in changing the relative energies of the two species. We next consider the possibility of oxidation of the CO-down orientation of formate, which strongly binds to Pt(111). We examine the difference between the oxidation reaction of the CH-down formate, versus the non-Faradaic adsorption of the CO-down formate, and

consider the roles of voltage and charge in these two processes. We then address how the oxidation reaction barrier changes under likely experimental surface conditions, by expanding our consideration of solvation effects through the inclusion of an explicit water molecule, and investigating the role of adsorbates on the surface. We lastly explore the applicability of this reaction mechanism to other catalysts, through a comparison of the reaction on Au(111) and Pt(111).

#### 3.1 CH-down formate and formic acid

To investigate the pathway for Reaction 3, we performed a two-dimensional scan of the potential energy surface for the reaction of formate approaching the platinum surface with the C–H pointing towards a Pt atom as a function of the C and H positions relative to the surface. We interpolated the DFT energies and force projections in this two-dimensional space, and found an approximate minimum-energy path by directly solving for zero tangential forces. As shown in Figure 3, the formate reacts barrierlessly with Pt to produce CO<sub>2</sub> and adsorbed H at 0 V vs SHE. As formate approaches the surface, the C–H bond is broken, and H binds to Pt. Importantly, the formate does not bind to the surface as the first step of this reaction – only the H binds to the Pt. The surface is weakly repulsive towards CO<sub>2</sub>, which moves away with the slow decrease in energy seen in the bottom right of Figure 3. The free energies that we report include the contribution of the configurational entropy of the solvent, but they do not include the entropy contribution from molecular vibration. We performed a vibrational analysis at 0 V for the products and reactants to correct for this. The zero point energy changes the results by less than 0.01 eV. The entropy contribution at room temperature due to molecule vibration, which is not included in the reported approximate free energies, is 0.27 eV, and will cause a shift in the expected reversible potential for the reaction.

We compare the formate reaction at a given Pt–C distance (from the path shown in Figure 3), to that of formic acid through a relaxed energy scan of the formic acid with fixed C positions. Figure 4 depicts the binding and reaction energies of formate and formic acid relative to the energies of the respective solvated molecules plus the solvated platinum slab at 0 V vs. SHE. As shown in Figure 4, the formic acid approaches the clean Pt surface and does not react. The energy eventually increases slightly once the formic acid becomes too close to the Pt surface. In contrast, when the formate approaches the Pt surface with its H pointed towards the surface, it produces CO<sub>2</sub> and H bound to the surface, even at 0 V, with a net reaction energy of more than 1 eV. At each point in these scans, the CO<sub>2</sub> molecule is at a fixed position near the surface. When it is allowed to relax, the CO<sub>2</sub> moves away from the surface, and the minimum energy is –1.25 eV at 0 V. The finding that the C–H-down formic acid does not bind to the solvated platinum surface agrees with that of Wang and Liu.<sup>10</sup>

<sup>†</sup> If one wishes to compare to the results calibrated from the potential of zero charge,<sup>46</sup> the reported values should be shifted to account for a vacuum value of 4.68 V.

<sup>‡</sup> This is not true at very large distances, where the Fermi level will not match that of the slab, and a theory beyond density functional theory, such as constrained DFT, would be necessary to describe such systems.

<sup>§</sup> We extend our calculations up to 1 V to compare Pt(111) and Au(111), and we observed a linear relationship in the free energy of reaction through 1 V, and we do not see evidence of this possible destabilization at 1 V either.

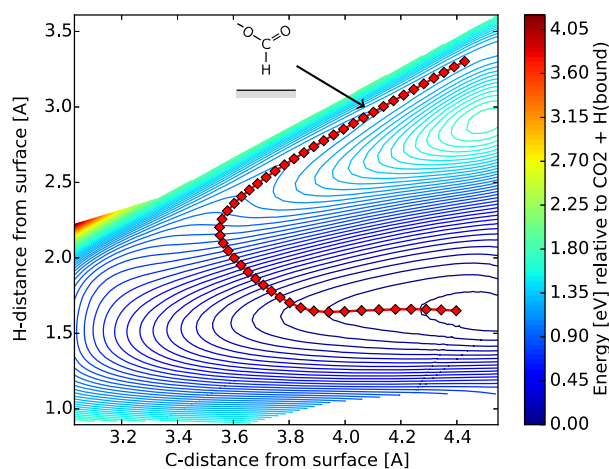


**Fig. 3** Contour plot of the potential energy as the C and H positions ( $\text{\AA}$ ) are scanned at 0 V vs. SHE. The reaction pathway is depicted in red.

However, it is striking that formate reacts with such a large energy and formic acid does not, given that the molecules only differ by a proton.

To more closely examine the relative reactivities of formic acid and formate, we consider the free energy difference between the two species as a function of pH. Figure 4 references the free energy of each species to its energy in solution, which allows for comparison between the two species only when these energies are equal, in other words, when the pH is equal to 3.77, the  $pK_a$  of formic acid. As the pH changes, the free energy of the formate (and a solvated proton, not included in the DFT calculation) at room temperature changes relative to that of formic acid, according to  $\Delta G = 0.059(pK_a - pH)$ , where a negative free energy change means that the formate is more stable than the formic acid ( $pH > pK_a$ ). At  $pH < pK_a$ , the formic acid will have a lower free energy, and will be present at higher concentrations. To make contact between experiments performed at  $pH = 1$  to  $pH = 2$ , we note that the formic acid will be 0.16 eV and 0.10 eV, respectively, more stable than formate. If the formic acid reaction barrier on the surface is larger than these values, we expect that the formate reaction will be the dominant one. Given that we predict a reaction barrier of at least this magnitude for the formic acid to directly react with the surface, we expect that the barrierless formate oxidation will dominate under these experimental conditions.

We note, however, that there is one more possibility – that the formic acid loses its proton as it nears the surface. This is difficult to assess with our implicit solvation scheme given the difficulty of accurately representing the solvated proton. We can see evidence that the  $pK_a$  of formic acid decreases as the formic acid

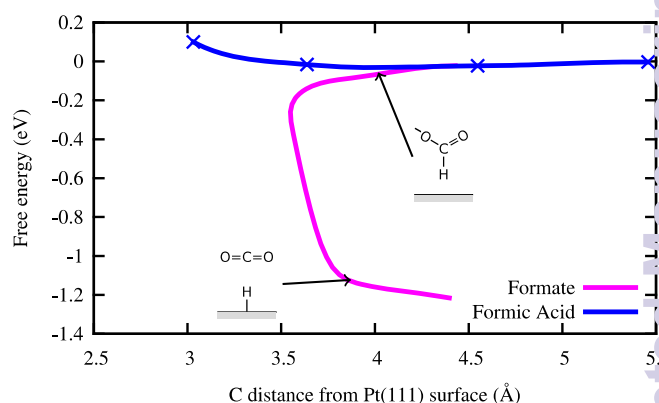


**Fig. 4** Relaxed energy scan of formic acid approaching a Pt surface with H down at 0 V, and energy along the minimum-energy reaction path for formate as a function of distance between the C and the nearest Pt. For the formic acid, the symbols depict the calculated energies, and the connecting line is a spline constructed using the calculated forces and energies.

approaches, because we can see the relative energy change in Figure 4, but we do not know the timescale associated with losing the proton relative to that of the approach of the species. However, if formic acid loses its proton while the formate oxidation reaction is barrierless, the formic acid reaction will have a barrier at least as high as the (pH dependent) reaction energy needed for deprotonation to form formate,  $\Delta G = 0.059(pK_a - pH)$ . This agrees well with experimental evidence that suggests that the reaction is first order with respect to formate concentration, especially at very low pH. However, the barrier associated with deprotonation of the formic acid followed by formate oxidation will be low when the  $pK_a$  equals the pH, so this process is at least plausible under certain experimental conditions, although it is a two step process.

### 3.2 O-down formate

While formate clearly reacts with Pt when H is facing the surface it can also be bound in the “bridged formate” configuration,<sup>54</sup> in which both O atoms bind to neighboring Pt atoms. The formate that adsorbs on the surface in this configuration acts as a poison preventing CH-down formate from reacting at a given platinum site. Figure 5 illustrates that as formate approaches Pt O-down it binds to the surface. As the voltage increases from 0 V to 0.5 V, the formate binds more strongly to the increasingly positive Pt surface. This binding process exhibits a barrier at 0 V vs SHE that is an order of magnitude larger than  $k_B T$  at standard operating temperatures, that decreases with increasing voltage. Others<sup>35</sup> have suggested that the adsorbed bridged formate form from formic acid, because the amount of bridged formate on the surface decreases with increasing pH. Our results indicate an alternate explanation, that at a fixed potential on the reversible h

drogen electrode scale (i.e. with a 0.059 V per decade decrease in voltage versus SHE with increasing pH), the barrier to adsorption increases as the pH increases, as illustrated in Figure 5.

This strongly-bound, bridged formate structure has a high barrier to dissociation from the Pt surface, and consequently a high barrier for oxidation (c.f., Ref. 36), because it must first become unbound from the surface. The finding that the formate strongly binds in the bridged formate configuration agrees well with recent experimental work,<sup>24</sup> which found that the formic acid oxidation current on Pt(111) is proportional to  $c_{\text{HCOOH}}(1 - 2\theta_f)$ , where  $\theta_f$  is the coverage of bridge-bonded formate, and  $c_{\text{HCOOH}}$  is the concentration of formic acid at the electrode surface. The pH dependence is not explored in that reference, so the reported rate dependence is indistinguishable from first-order dependence on formate, as expected in this work, proportional to  $c_{\text{HCOO}^-}(1 - \theta_a)$ , where  $(1 - \theta_a)$  represents the fraction of available Pt sites.

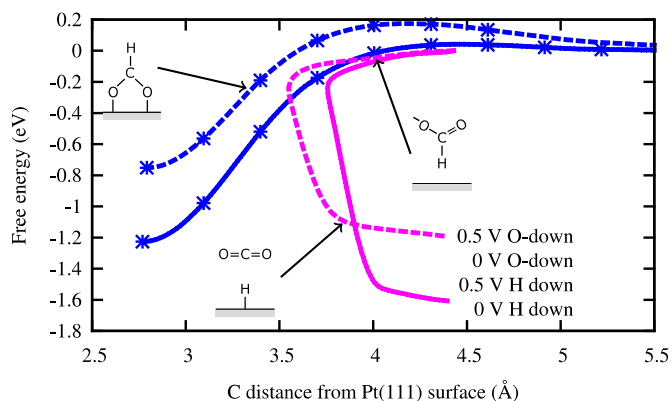


**Fig. 5** Relaxed energy scans of formate approaching a pristine Pt(111) surface in solution, in the O-down (blue lines) orientation, and energy along the minimum-energy reaction path for formate as function of C distance for the H-down reaction. The zero of the free energy is set to the sum of the energies of the formate in solution and the solvated metal surface.

To more clearly illustrate the difference between the formate oxidation and the interaction of the bridged formate with the catalyst, Figure 6 shows the change in charge as the two differently oriented formate anions and the formic acid approach the surface. Mirroring the experimental conditions, the charge of the system (i.e. the cell containing the slab, formate, and fluid) changes as species approach the surface, since the calculations are performed at fixed potential. As O-down formate approaches the surface, excess negative charge slowly decreases as the surface responds to the approach of negatively-charged O atoms. In contrast, as H-down formate approaches the surface, the charge of the system does not drastically change until the formate is oxidized and H binds to the surface. Then the transferred electron leaves the system. As expected, both ion transfer reactions become more

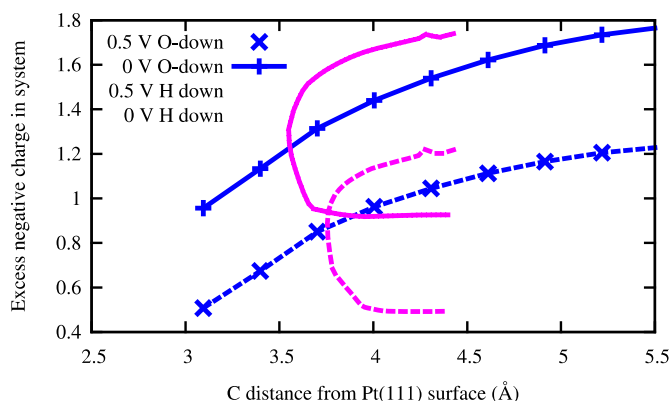


**Fig. 6** System charge as a function of C distance. As the O-down formate binds to the Pt, the charge state of the system changes gradually during the non-Faradaic process. In contrast, as the H-down formate reacts, a sharp drop in excess negative charge is seen once the reaction occurs.

favorable with increased voltage.

### 3.3 Formate solvation

While the direct oxidation of formate seems like a favorable mechanism for the formic acid oxidation reaction, we need to evaluate the interaction between formate and explicit water to be more certain. A correct description of water is particularly important for the formate anion which can form strong hydrogen bonds with liquid water. Most implicit solvation models underestimate the solvation energies of anions in water. The solvation model used in this work<sup>46</sup> predicts the formate solvation energy to be 2.83 eV, compared to the experimental value of 3.28 eV.<sup>55</sup> This effect shifts the reversible potential of formate oxidation, and decreases the reaction energies in Figures 3, 4, and 5 by 0.45 eV, but the important question is whether this reaction will now have a reaction barrier. To address this, we consider an explicit water molecule, interacting with one of the oxygens of the H-down formate. We chose the placement of this water molecule so that it may strongly hydrogen bond with the formate oxygen. As shown in Figure 7, the addition of an explicit water molecule decreases the reversible potential for the reaction, as expected, because the explicit water further stabilizes formate, but does not particularly stabilize the CO<sub>2</sub> or adsorbed H. However, the reaction still proceeds in the same way: although the formate is now more stabilized, the hydrophobic region of formate containing the C–H is still available for reaction.

The above results suggest that calculations with multiple explicit water molecules, hydrogen-bound to the formate, will not lead to a barrier. As long as formate reacts directly from solution and does not first adsorb on the surface, the reaction appears to proceed barrierlessly. However, a small barrier could potentially

be introduced by the need for a water molecule that solvates the platinum surface to move out of the path of the approaching formate. This result contrasts with the findings of Wang and Liu that monodentate formate will oxidize on a Pt surface with a barrier of less than 0.05 eV in vacuum, but with a barrier approximately 1 eV in a solvated environment.<sup>10</sup> On the other hand, the reaction of O-down formate differs significantly from the H-down oxidation process. Both the water and the surface interact with the O atom in formate, and we therefore expect that the barrier depicted in Figure 5 for the binding of bridged formate is underestimated.

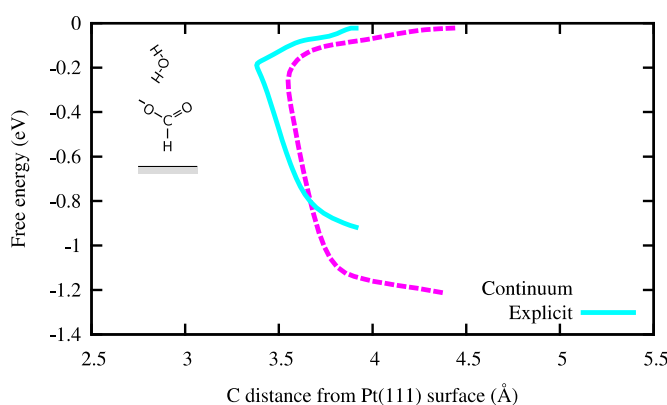


**Fig. 7** Energy along the minimum-energy reaction path for formate approaching Pt(111) H-down, with and without an explicit water molecule.

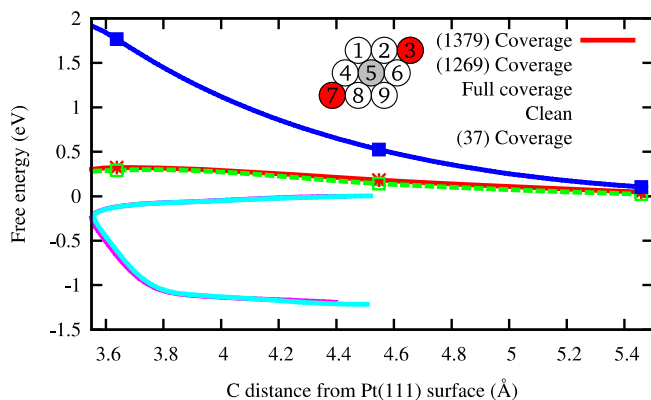


**Fig. 8** Relaxed energy scans and energy along the minimum-energy reaction paths, showing the binding energy of formate approaching Pt(111) at 0 V, with differing coverages of CO, splined using the force data. Indices indicate coverage, with (37) coverage illustrated above, and "Full coverage" indicating coverage on all but site 5, the Pt reaction site.

### 3.4 Reaction 3 and surface adsorbates

We next consider the effect of surface adsorbates on Reaction 3 to determine if the reaction remains barrierless under more realistic operating conditions. To mimic CO coverage effects, we examined different coverages of CO on the Pt(111) surface. Figure 8 shows that increasing amounts of CO on the Pt surface indeed created barriers for reaction at Pt atoms adjacent to the surface-covered sites, consistent with the well-known ability of CO to block the surface (c.f., Ref. 56). Additionally, the hydrogen adsorption energy decreases for these CO covered surfaces relative to pristine Pt, for instance by 0.25 eV for the (1379) coverage (following the notation for the coverage shown in Figure 8) at 0 V, suggesting that both site-blocking and electronic effects play a role in surface poisoning. Poisoning is expected to be important for not only CO but for other surface adsorbates as well, meaning that the reaction rate will depend on the number of sites available for reaction and the surface coverage on neighboring atoms.

The barrierless nature of Reaction 3 leads us to consider why the reaction onset is experimentally observed at higher than expected voltages. Two processes may prevent the reaction's onset. First, underpotential deposited H ( $H_{\text{upd}}$ ), present at voltages up to about 0.2 V,<sup>57</sup> passivates the Pt surface, with behavior similar to CO (see Supporting Information). Given the reversal symmetry of the  $H_{\text{upd}}$  waves seen in cyclic voltammetry, the rate of  $H_{\text{upd}}$  desorption is known to be fast, and so this is a thermodynamic effect. Additionally, Reaction 4 must be energetically favorable for the reaction to proceed. The energetics of this reaction are related to the phenomenon of  $H_{\text{upd}}$  on the surface, but are a separate effect, especially considering that  $H_{\text{upd}}$  is expected to mostly reside on fcc sites, whereas the H from Reaction 4 is initially on atop sites. We note that  $H_{\text{upd}}$  coverage is significantly reduced in the presence of adatoms, and we suggest that changes in H binding strength could explain the earlier onset of formic acid oxidation on adatom-modified Pt surfaces, rather than the recently proposed steering mechanism.<sup>38</sup>

This study captures the importance of the thermodynamic stability of adsorbed intermediates in the formic acid oxidation process. At low voltages, we expect Reaction 4 to be rate limiting, with the additional effect of increased barriers of Reaction 3. At higher voltages, and a pH below the  $pK_a$  of formate, we expect Reaction 2 to limit the rate. The real Pt surface that is probed experimentally under electrocatalytic conditions will have adsorbates including  $H_{\text{upd}}$ , strongly adsorbed water molecules, anionic species such as  $\text{Cl}^-$  and  $\text{OH}^-$ , and bridged formate on the surface, for instance. Under these conditions, we expect the availability of Pt sites to be rate limiting.

The results suggest that formic acid oxidation happens through the reaction of formate with the Pt surface, to produce  $\text{CO}_2$  and adsorbed H, which is subsequently oxidatively desorbed. Invoking the steady state approximation for formate/formic acid and



potential (vs. SHE)	Au(111)	Pt(111)
0 V	-0.47	-1.25
0.5 V	-0.88	-1.66
1 V	-1.22	-2.02

**Table 1** Reaction energies (eV) for Reaction 3 for Au(111) and Pt(111). We note that the magnitudes of the reaction energies here are considerably lowered by the inclusion of additional solvation (0.45 eV) and entropy (0.27 eV for Pt(111)) terms.

the H adsorption/desorption processes, the dependence of the rate on pH leads to an oxidation current plateau at the  $pK_a$  of formate (see Supporting Information). This is supported by the experimental work of Brimaud et al.,<sup>35</sup> but not by Joo et al.,<sup>25</sup> who find that the oxidation current peaks at the  $pK_a$  of formate. Joo et al. conclude that their observation is a function of Pt surface oxidation at higher pH, although they discuss the possibility of other sources of pH dependence.<sup>58</sup>

### 3.5 Reaction 3 on Au(111)

Lastly, we compare the behavior of formic acid oxidation on Pt with that on Au, to evaluate the general applicability of this reaction mechanism to other metal surfaces and to see if the H binding strength of Pt plays a large role in determining the reversible potential of Reaction 3. Au provides a well-studied<sup>31,59–64</sup> counterpoint to Pt, as it binds less strongly to H. Table 1 demonstrates the striking difference between Pt and Au, with a much smaller reaction energy on Au(111). Experimentally, a much smaller current is observed on Au(111) surfaces, and the onset of reaction happens at a higher potential.<sup>35</sup> Despite the barrierless nature of the reaction, the stabilization of the H on the surface may be too low for the reaction to proceed at low voltages, once the solvation energy corrections (0.45 eV) and vibrational energies are taken into account. The modest free energies for this reaction suggest that the onset of reaction on Au may be dominated by Reaction 3 rather than by Reaction 4, which likely limits the reaction onset on Pt, as illustrated in Figure 9. For the Au surface, this reaction mechanism may not be the primary one, and other mechanisms involving adsorbates that stabilize the H should be considered.

## 4 Conclusion

We provide evidence that formate reacts barrierlessly on clean platinum in the CH-down configuration to produce  $\text{CO}_2$  and adsorbed hydrogen, and the results support the notion that formate must be considered as a reactant to capture the behavior seen in experiments. The results suggest that the formate does not need to adsorb to react with the platinum surface, and that adsorbants poison the catalyst by blocking active sites. They demonstrate the need to carefully evaluate all of the contributions to the free

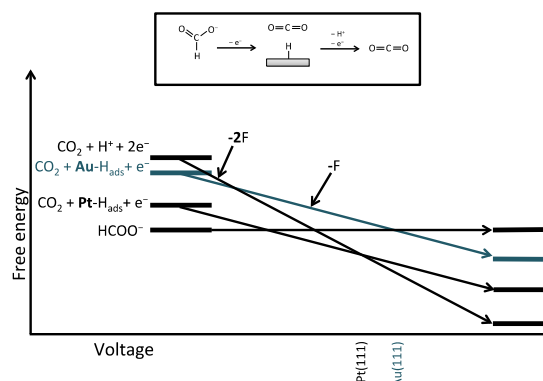


**Fig. 9** Relative energies of products, reactants, and intermediates of the formic acid oxidation reaction on Pt(111) and on Au(111) as a function of voltage. The arrows identify the slopes of the lines, where  $F$  is Faraday's constant. The dotted lines indicate the onset of reaction, with the onset of reaction on Pt(111) limited by the desorption of H, and the onset of reaction on Au(111) limited by the stabilization of the  $\text{H}_{\text{ads}}$

energy for the reactants and products. Inclusion of entropy, solvation, voltage and pH effects is particularly important for the formic acid oxidation reaction. This allows for improved comparisons between computation and experiments, and permits evaluation of a larger set of possible reactants and reaction mechanisms.

The overall formic acid oxidation reaction is controlled by Reactions 2, 3 and 4. The free energy associated with Reaction 2 changes with the solution pH, and is not directly affected by the voltage. In contrast, the reaction energy for Reactions 3 and Reaction 4 change with voltage. We expect the desorption of hydrogen, Reaction 4, to limit the overall reaction rate at low voltages.

The results additionally provide an explanation as to why an active surface intermediate for the direct formic acid oxidation reaction has not been found. Experimental work has probed the surface for this intermediate, yet evidence for it is lacking. If the formate reacts upon approach to the surface, and the only resulting surface adsorbate is the hydrogen, then this active surface intermediate will not be identified by current spectroscopic approaches. Future experimental work to probe the coverage of adsorbed hydrogen on the surface, as a result of the formic acid oxidation reaction, would provide further insight.

## 5 Acknowledgement

KAS acknowledges funding from the NIST-NRC postdoctoral program. RS was supported by the Joint Center for Artificial Photosynthesis, a DOE Energy Innovation Hub, supported through the Office of Science of the U.S. Department of Energy under Award Number DE-SC0004993

## References

- 1 P. G. Grimes and H. M. Spengler, *Hydrocarbon Fuel Cell Technology*, Academic Press, New York, 1965, p. 121.
- 2 Y. Zhu, S. Y. Ha and R. I. Masel, *J. Power Sources*, 2004, **130**, 8–14.
- 3 S. Ha, B. Adams and R. I. Masel, *J. Power Sources*, 2004, **128**, 119–124.
- 4 S. Ha, R. Larsen and R. I. Masel, *J. Power Sources*, 2005, **144**, 28–34.
- 5 Y. Zhu, Z. Khan and R. I. Masel, *J. Power Sources*, 2005, **139**, 15–20.
- 6 S. Ha, Z. Dunbar and R. I. Masel, *J. Power Sources*, 2006, **158**, 129–136.
- 7 R. Larsen, S. Ha, J. Zakzeski and R. I. Masel, *J. Power Sources*, 2006, **157**, 78–87.
- 8 C. Rice, S. Ha, R. I. Masel, P. Waszczuk, A. Wieckowski and T. Barnard, *J. Power Sources*, 2002, **111**, 83–89.
- 9 M. Neurock, M. Janik and A. Wieckowski, *Faraday Discuss.*, 2009, **140**, 363–378.
- 10 H. F. Wang and Z. P. Liu, *J. Phys. Chem. C*, 2009, **113**, 17502–17508.
- 11 B. C. Batista and H. Varela, *J. Phys. Chem. C*, 2010, **114**, 18494–18500.
- 12 W. Gao, J. A. Keith, J. Anton and T. Jacob, *J. Am. Chem. Soc.*, 2010, **132**, 18377–18385.
- 13 A. Capon and R. Parsons, *J. Electroanal. Chem. Interfacial Electrochem.*, 1973, **45**, 205–231.
- 14 S. Sun and J. Clavilier, *J. Electroanal. Chem. Interfacial Electrochem.*, 1987, **240**, 147–159.
- 15 Y. X. Chen, S. Ye, M. Heinen, Z. Jusys, M. Osawa and R. J. Behm, *J. Phys. Chem. B*, 2006, **110**, 9534–9544.
- 16 G. Samjeské, A. Miki, S. Ye, A. Yamakata, Y. Mukoyama, H. Okamoto and M. Osawa, *J. Phys. Chem. B*, 2005, **109**, 23509–23516.
- 17 G. Samjeské and M. Osawa, *Angew. Chem., Int. Ed.*, 2005, **44**, 5694–5698.
- 18 G. Samjeské, A. Miki, S. Ye and M. Osawa, *J. Phys. Chem. B*, 2006, **110**, 16559–16566.
- 19 Y. Mukoyama, M. Kikuchi, G. Samjeské, M. Osawa and H. Okamoto, *J. Phys. Chem. B*, 2006, **110**, 11912–11917.
- 20 Y. X. Chen, S. Ye, M. Heinen, Z. Jusys, M. Osawa and R. J. Behm, *Langmuir*, 2006, **22**, 10399–10408.
- 21 Y. X. Chen, M. Heinen, Z. Jusys and R. J. Behm, *Angew. Chem., Int. Ed.*, 2006, **45**, 981–985.
- 22 Y. X. Chen, M. Heinen, Z. Jusys and R. J. Behm, *ChemPhysChem*, 2007, **8**, 380–385.
- 23 M. Osawa, K. i. Komatsu, G. Samjeské, T. Uchida, T. Ikeshoji, A. Cuesta and C. Gutiérrez, *Angew. Chem., Int. Ed.*, 2011, **50**, 1159–1163.
- 24 J. Xu, D. Yuan, F. Yang, D. Mei, Z. Zhang and Y.-X. Chen, *Phys. Chem. Chem. Phys.*, 2013, **15**, 4367–4376.
- 25 J. Joo, T. Uchida, A. Cuesta, M. T. M. Koper and M. Osawa, *J. Am. Chem. Soc.*, 2013, **135**, 9991–9994.
- 26 E. Müller, *Z. Electrochem.*, 1923, **29**, 264–274.
- 27 E. Müller, *Z. Electrochem.*, 1927, **33**, 561–568.
- 28 E. Müller and S. Tanaka, *Z. Electrochem.*, 1928, **34**, 256–264.
- 29 J. Perales-Rondon, E. Herrero and J. Feliu, *J. Electroanal. Chem.*, 2015, **742**, 90–96.
- 30 E. Bertin, A. Fleury, C. Roy, M. Martin, S. Garbarino and D. Guay, *Electrochim. Acta*, 2015, **162**, 237–244.
- 31 A. Cuesta, G. Cabello, M. Osawa and C. Gutiérrez, *ACS Catal.*, 2012, **2**, 728–738.
- 32 A. Cuesta, G. Cabello, F. W. Hartl, M. Escudero-Escribano, C. Vaz-Dominguez, L. A. Kibler, M. Osawa and C. Gutiérrez, *Catal. Today*, 2013, **202**, 79–86.
- 33 J. Joo, T. Uchida, A. Cuesta, M. Koper and M. Osawa, *Electrochim. Acta*, 2014, **129**, 129–136.
- 34 J. V. Perales-Rondon, E. Herrero and J. Feliu, *Electrochim. Acta*, 2014, **140**, 511–517.
- 35 S. Brimaud, J. Solla-Gullon, I. Weber, J. Feliu and R. J. Behm, *ChemElectroChem*, 2014, **1**, 1075–1083.
- 36 M. Neurock, M. Janik and A. Wieckowski, *Faraday Discussions*, 2008, **140**, 363–378.
- 37 W. Gao, E. Song, Q. Jiang and T. Jacob, *Chem. Eur. J.*, 2014, **20**, 11005–11012.
- 38 J. V. Perales-Rondon, A. Ferre-Vilaplana, J. Feliu and E. Herrero, *J. Am. Chem. Soc.*, 2014, **136**, 13110–13113.
- 39 M. Nielsen, M. E. Bjorketun, M. H. Hansen and J. Rossmeisl, *Surf. Sci.*, 2015, **631**, 2–7.
- 40 K. Letchworth-Weaver and T. Arias, *Phys. Rev. B*, 2012, **85**, 075140.
- 41 J. K. Nørskov, J. Rossmeisl, A. Logadottir, L. Lindqvist, J. R. Kitchin, T. Bligaard and H. Jonsson, *J. Phys. Chem. B*, 2004, **108**, 17886–17892.
- 42 F. Gossenbergera, T. Romana and A. Gross, *Surf. Sci.*, 2015, **631**, 17–22.
- 43 C. Taylor, S. Wasileski, J. Filhol and M. Neurock, *Phys. Rev. B*, 2006, **73**, 165402.
- 44 S. Ismail-Beigi and T. Arias, *Comp. Phys. Comm.*, 2000, **128**, 1–45.
- 45 S. Petrosyan, A. Rigos and T. Arias, *J. Phys. Chem. B*, 2005, **109**, 15436.
- 46 D. Gunceler, K. Letchworth-Weaver, R. Sundararaman, K. Schwarz and T. Arias, *Modelling Simul. Mater. Sci. Eng.*, 2013, **21**, 074005.
- 47 R. Sundararaman, K. Schwarz, K. Letchworth-Weaver and

- T. Arias, *J. Chem. Phys.*, 2015, **142**, 054102.
- 48 R. Sundararaman and W. Goddard, *J. Chem. Phys.*, 2015, **142**, 064107.
- 49 R. Sundararaman, K. Letchworth-Weaver, K. A. Schwarz and T. Arias, *JDFTx*, 2012, <http://jdftx.sourceforge.net/>, last accessed May 2015.
- 50 J. Perdew, K. Burke and M. Ernzerhof, *Phys. Rev. Lett.*, 1996, **77**, 3865–3868.
- 51 C. A. Rozzi, D. Varsano, A. Marini, E. K. U. Gross and A. Rubio, *Phys. Rev. B*, 2006, **73**, 205119.
- 52 R. Sundararaman and T. Arias, *Phys. Rev. B*, 2013, **87**, 165122.
- 53 C. Freysoldt, S. Boeck and J. Neugebauer, *Phys. Rev. B*, 2009, **79**, 241103(R).
- 54 A. Miki, S. Ye, T. Senzaki and M. Osawa, *J. Electroanal. Chem.*, 2004, **563**, 23–31.
- 55 J. Pliego and J. Riveros, *Phys. Chem. Chem. Phys.*, 2002, **4**, 1622–1627.
- 56 N. M. Markovic, H. A. Gasteiger, P. N. Ross, X. Jiang, I. Villegas and M. J. Weaver, *Electrochim. Acta*, 1995, **40**, 91–98.
- 57 T. Tan, L. Wang, D. Johnson and K. Bai, *J. Phys. Chem. C*, 2013, 22696–22704.
- 58 M. Koper, *Chem. Sci.*, 2013, **4**, 2710–2723.
- 59 A. Capon and R. Parsons, *J. Electroanal. Chem.*, 1973, **44**, 239–254.
- 60 J. O. Besenhard, R. Parsons and R. M. Reeves, *J. Electroanal. Chem.*, 1979, **96**, 52–72.
- 61 A. Hamelin, Y. Ho, S.-C. Chang, X. Gao and M. J. Weaver, *Langmuir*, 1992, **8**, 975–981.
- 62 Y. Zhang and M. J. Weaver, *Langmuir*, 1993, **9**, 1397–1403.
- 63 J. Xiang, B.-L. Wu and S.-L. Chen, *J. Electroanal. Chem.*, 2001, **517**, 95–100.
- 64 G. L. Beltramo, T. E. Shubina and M. T. M. Koper, *ChemPhysChem*, 2005, **5**, 2597–2606.